General Disclaimer

One or more of the Following Statements may affect this Document

- This document has been reproduced from the best copy furnished by the organizational source. It is being released in the interest of making available as much information as possible.

- This document may contain data, which exceeds the sheet parameters. It was furnished in this condition by the organizational source and is the best copy available.

- This document may contain tone-on-tone or color graphs, charts and/or pictures, which have been reproduced in black and white.

- This document is paginated as submitted by the original source.

- Portions of this document are not fully legible due to the historical nature of some of the material. However, it is the best reproduction available from the original submission.

NUMERICAL SIMULATION OF WEATHER AND CLIMATE

Technical Report No. 5

NUMERICAL SIMULATION OF THE CLUSTERING OF CONSTANT-VOLUME BALLOONS IN THE GLOBAL DOMAIN

by

Fedor Mesinger and Yale Mintz

Sent for DRF

1 February 1970

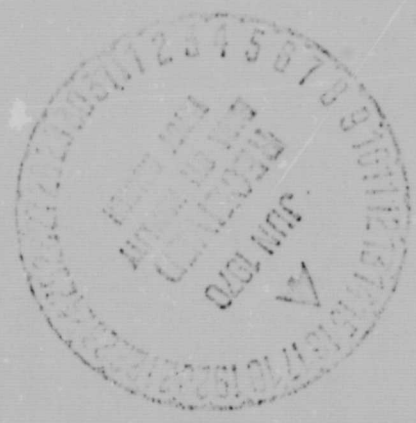

Department of Meteorology

University of California, Los Angeles

NUMERICAL SIMULATION OF WEATHER AND CLIMATE

Technical Report No. 5

NUMERICAL SIMULATION OF THE CLUSTERING OF CONSTANT-VOLUME BALLOONS IN THE GLOBAL DOMAIN

by

Fedor Mesinger and Yale Mintz

1 February 1970

Department of Meteorology

University of California, Los Angeles

TABLE OF CONTENTS

1. INTRODUCTION

The planning of the First GARP Global Experiment (FGGE) includes a subsystem of superpressure balloons. Earth orbiting satellites will track the motion of the balloons and communicate with sensors on them, and thereby provide measurements of the wind, temperature, pressure and geopotential of the air at the position of each balloon (cf. Lally and Lichfield, 1969; Morel, 1969). This FGGE plan (WMO-ICSU, 1969, section 4.1.2.4) calls for global coverage of balloons near the 200 mb level; and tropical coverage of balloons near the 900 mb level. These levels were chosen to provide measurements which have two degrees of freedom in the vertical in the tropical troposphere; and to avoid, in all latitudes, the failure of balloons by icing in supercooled water clouds.

The efficiency of the proposed balloon subsystem will greatly depend on the rate at which the balloons will cluster (or collect) as a consequence of the large scale horizontal velocity convergence at the balloon levels. In addition, some balloons at the 900 mb level will be lost by collision with the earth's surface.

It will be useful to have an advance estimate of the space-time balloon distribution which will result from the clustering and topographic collisions. The rate at which balloons are systematically removed from certain regions will determine the rate at which it will be necessary to release additional balloons into those regions in order to maintain the desired coverage.

Three prior studies have been made of the clustering of superpressure (constant-volume) balloons. In the first of these, Mesinger (1965) calculated the trajectories of balloons at 300 and 800 mb with winds obtained from the solution of the balance-equation and the omega-equation, as applied to observed Northern Hemisphere mass fields at 12 hourly intervals. Assuming initially randomly

distributed balloons, he calculated their trajectories for 30 days and determined the clustering rates at the two levels. Angell and Hass (1966) made a similar calculation for balloons at the 500 mb level, for several 60-day periods.

The above two studies showed only small rates of balloon clustering. However, the determination of the divergent wind component from the solution of the omega-equation is not very reliable. In addition, because these studies used the quasi-geostrophic approximation, the deformation wind component may have had large errors near the low latitude boundaries. Because the rate of balloon clustering depends on the difference between the opposing effects of the divergent component and the deformation component of the wind field, an error in one or both of these may make the clustering calculation unreliable. Furthermore, the above two studies were limited to the Northern Hemisphere, north of about 15^{o} latitude.

The third study, by Mintz (NAS-NRC, 1966, pp. 90-93), used the winds generated in a numerical simulation of the global atmospheric circulation with a two-level primitive equations model (Mintz, 1965). In the tropics at 800 mb, the balloons were carried by the north-easterly and south-easterly trade winds and clustered within the intertropical convergence zone. In the upper troposphere (400 mb), the balloons moved out of the tropics of both hemispheres and clustered along the middle latitude jet streams of the two hemispheres. Poleward of these jet streams, the balloon distributions were much less uniform than in the studies by Mesinger and Angell and Hass.

Since 1966, the above numerical model for simulating the global atmospheric circulation has been improved in several ways. The most important change was the addition of water vapor as a time-dependent variable, with Arakawa's parameterization of cumulus convection (Arakawa, Katayama and Mintz, 1969). This has produced a more realistic simulation of the atmospheric circulation in the

tropical region. There are now large perturbations in the tropical flow, so that the Hadley circulation varies with longitude. The new model also has an improved finite-difference scheme and a greater horizontal resolution (a grid size of 5^{o} longitude by 4^{o} of latitude), and it simulates middle latitude baroclinic disturbances fairly realistically.

The new numerical model was used for our numerical simulation of the 1970-71 Eole Experiment (Mesinger and Mintz, 1970). In section 2 of that study, we described the general properties of the model; and, in section 6, we showed a test comparison of the space-time distribution of observed GHOST balloons (Solot, 1968) with numerically simulated GHOST balloons, for the same season and initial locations. The good agreement between the observed and the simulated balloons as well as the realistic day-to-day synoptic fields generated in the numerical simulation, suggest that the global atmospheric circulation produced with the new model is realistic enough to give a fairly reliable estimate of the clustering of constant-volume balloons in the real atmosphere. Therefore, this new model was used to simulate the clustering of constant-volume balloons in the global domain, as described in the following sections of this report.

2. GLOBAL DISTRIBUTION OF BALLOONS IN THE UPPER TROPOSPHERE

To simulate the balloons at the proposed FGGE upper tropospheric level, we use the surface of constant air density, $\rho_2 = 0.329$ kg/m^3, which is the air density at 200 mb in the Standard Atmosphere. The location of this density surface and the wind field on this surface, as functions of space and time, are obtained as described in section 3 of the preceding report (Mesinger and Mintz, 1970).

The initial time for the global balloon simulation was taken as 0.0 GMT, December 1, year 1, in the model atmosphere. This is the same as the initial time in our numerical simulation of the 1970-71 Eole Experiment.

In the global simulation, we assume 3000 balloons at the level ρ_2, of which 1000 are initially randomly distributed within each one-third of the globe: 90°S to 19.5°S; 19.5°S to 19.5°N; and 19.5°N to 90°N. These are respectively designated as the A, B and C balloons. By assigning an equal number of balloons to each one-third of the globe, the global distribution becomes only approximately, rather than exactly random. From their locations at the initial time, the trajectories of the balloons were calculated for 90 days (ending 0.0 GMT, March 1, year 2, in the model atmosphere.) The trajectories were computed with the numerical scheme that is described in section 3 of the preceding report.

Figures 1 through 10 show the global distributions of the balloons, at 10 day intervals, on equal area polar projections of the Northern and Southern Hemispheres. To have the balloon designators legible, and also printed close to their true locations, only 1000 of the 3000 balloons are shown on the maps. (The 1000 balloons shown are also initially randomly distributed within each one-third of the area of the globe.) Because the positioning of a balloon on the map is constrained by the resolution of the line-printer, if two balloons fall within the same printing location the second balloon (and, more rarely, others too) is printed in the nearest vacant printing space at one or the other side, or below the true printing location.

Figure 1 shows the initial positions of the 1000 balloons. Even with the given random distribution (which gives the same probability of having a balloon within any small unit area), we obtain a few moderately large regions without any balloons: for example, in the Southern Hemisphere middle latitudes near

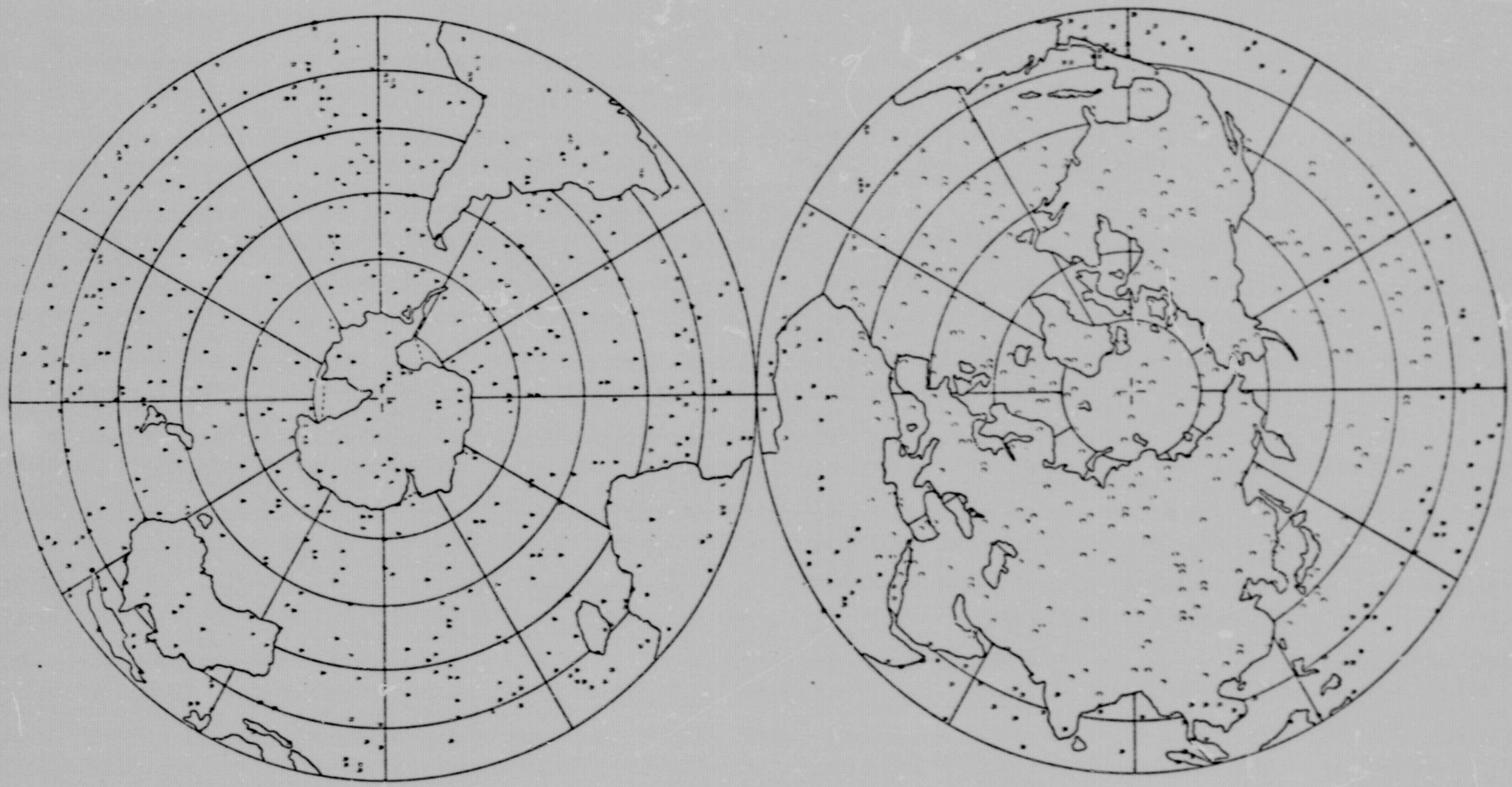

Fig. 1. Balloon positions at the upper level, on polar equal area projections, at day 0.0.

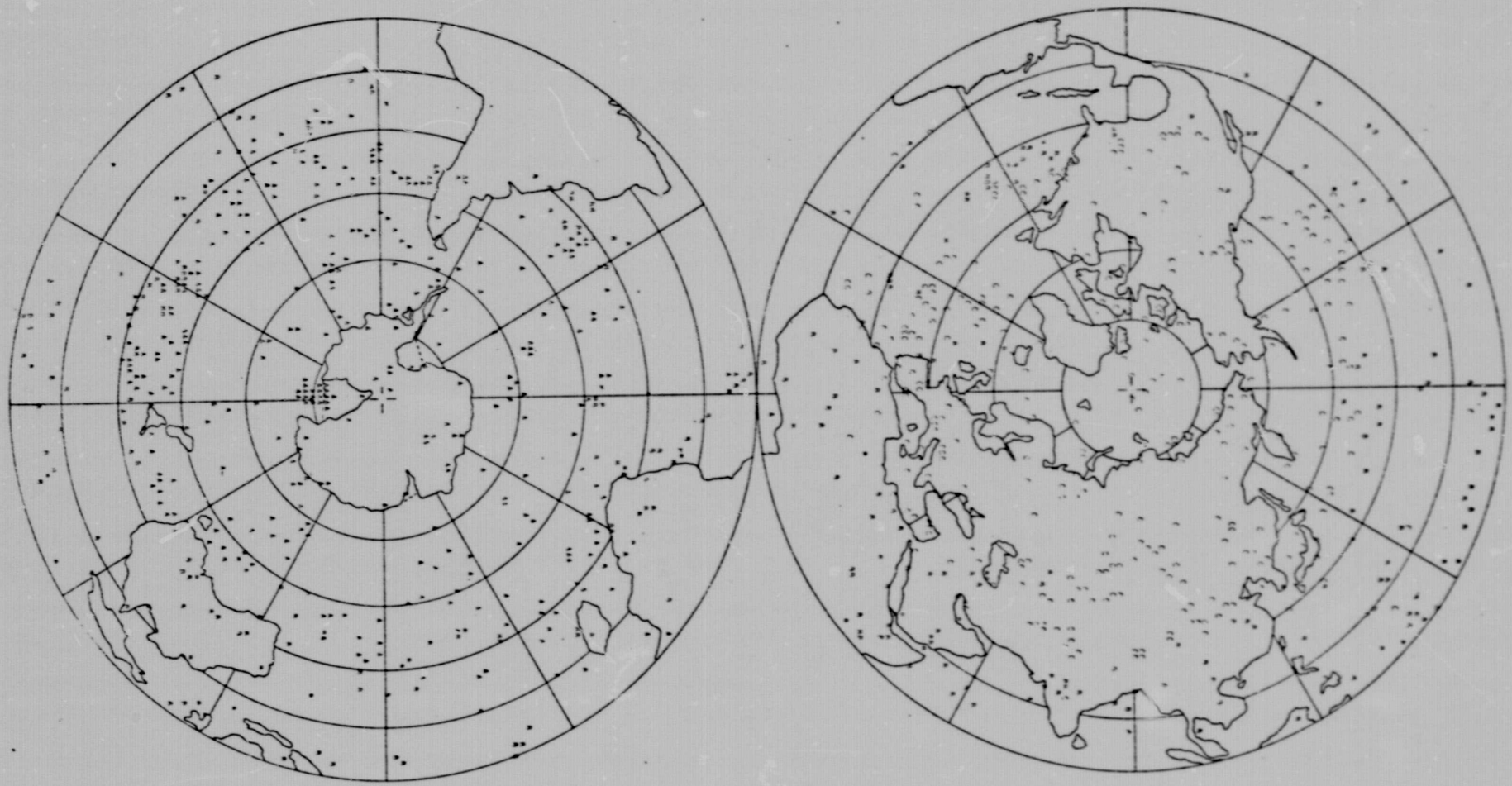

Fig. 2. Balloon positions at the upper level, on polar equal area projections, at day 10.

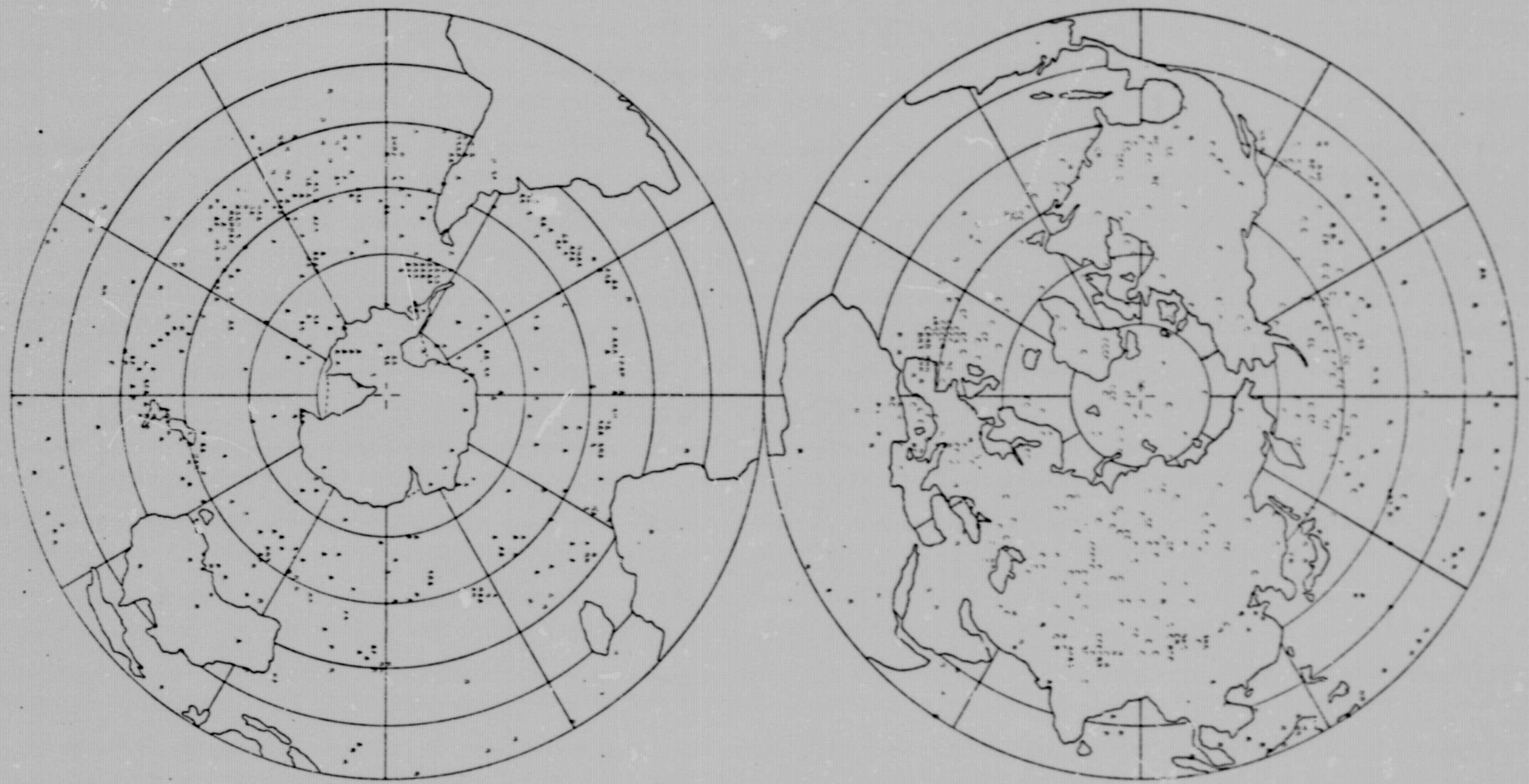

Fig. 3. Balloon positions at the upper level, on polar equal area projections, at day 20.

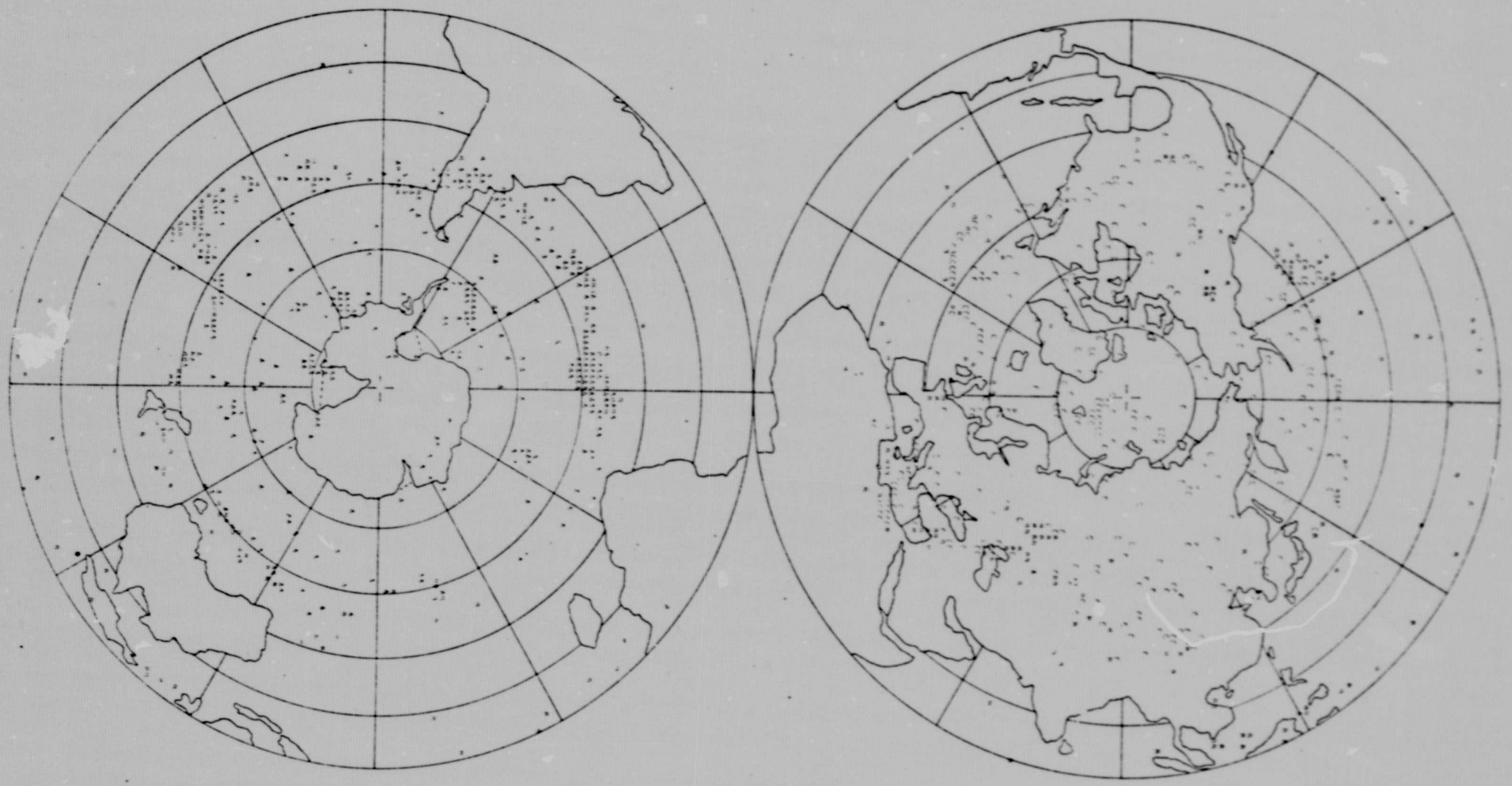

Fig. 4. Balloon positions at the upper level, on polar equal area projections, at day 30.

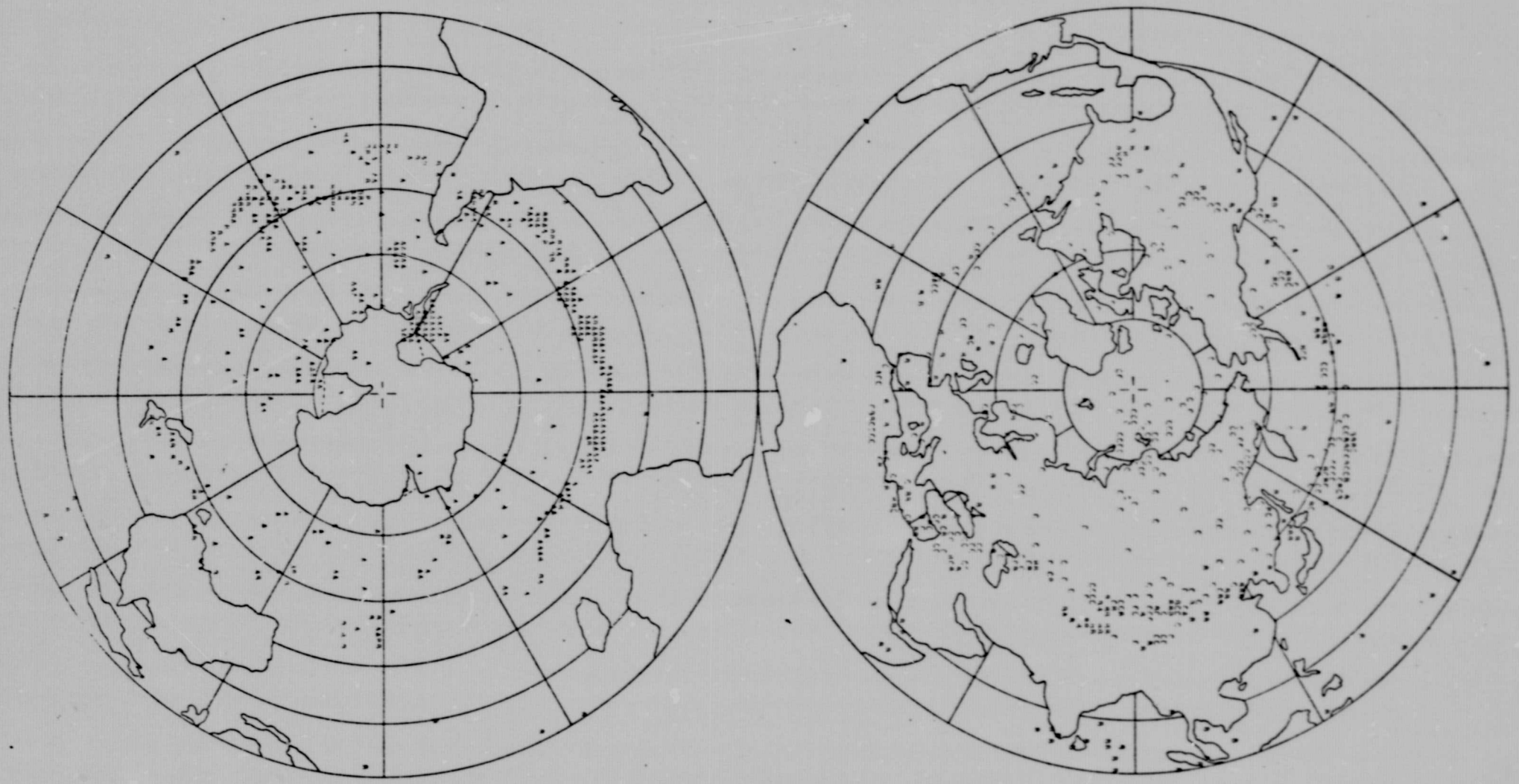

Fig. 5. Balloon positions at the upper level, on polar equal area projections, at day 40.

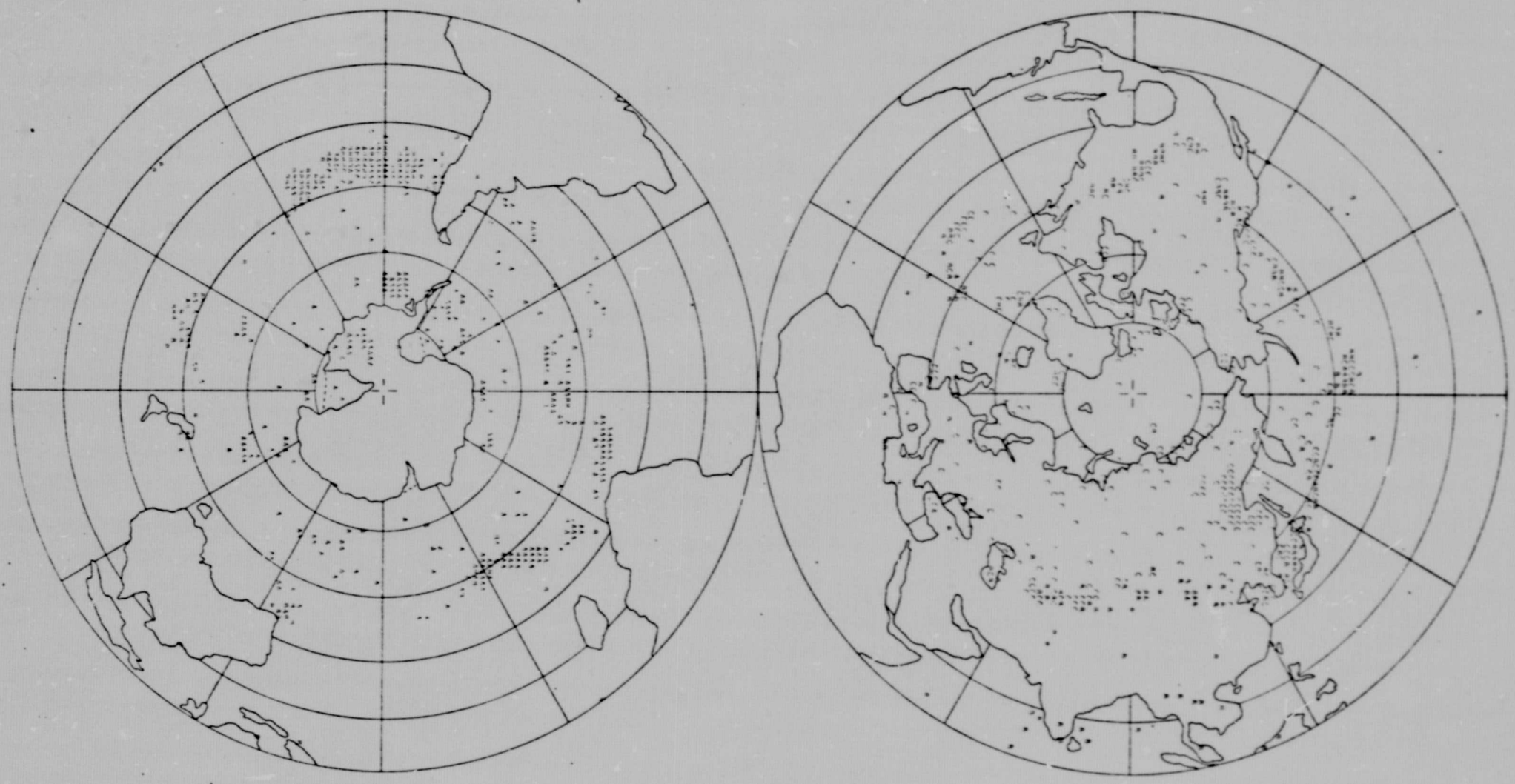

Fig. 6. Balloon positions at the upper level, on polar equal area projections, at day 50.

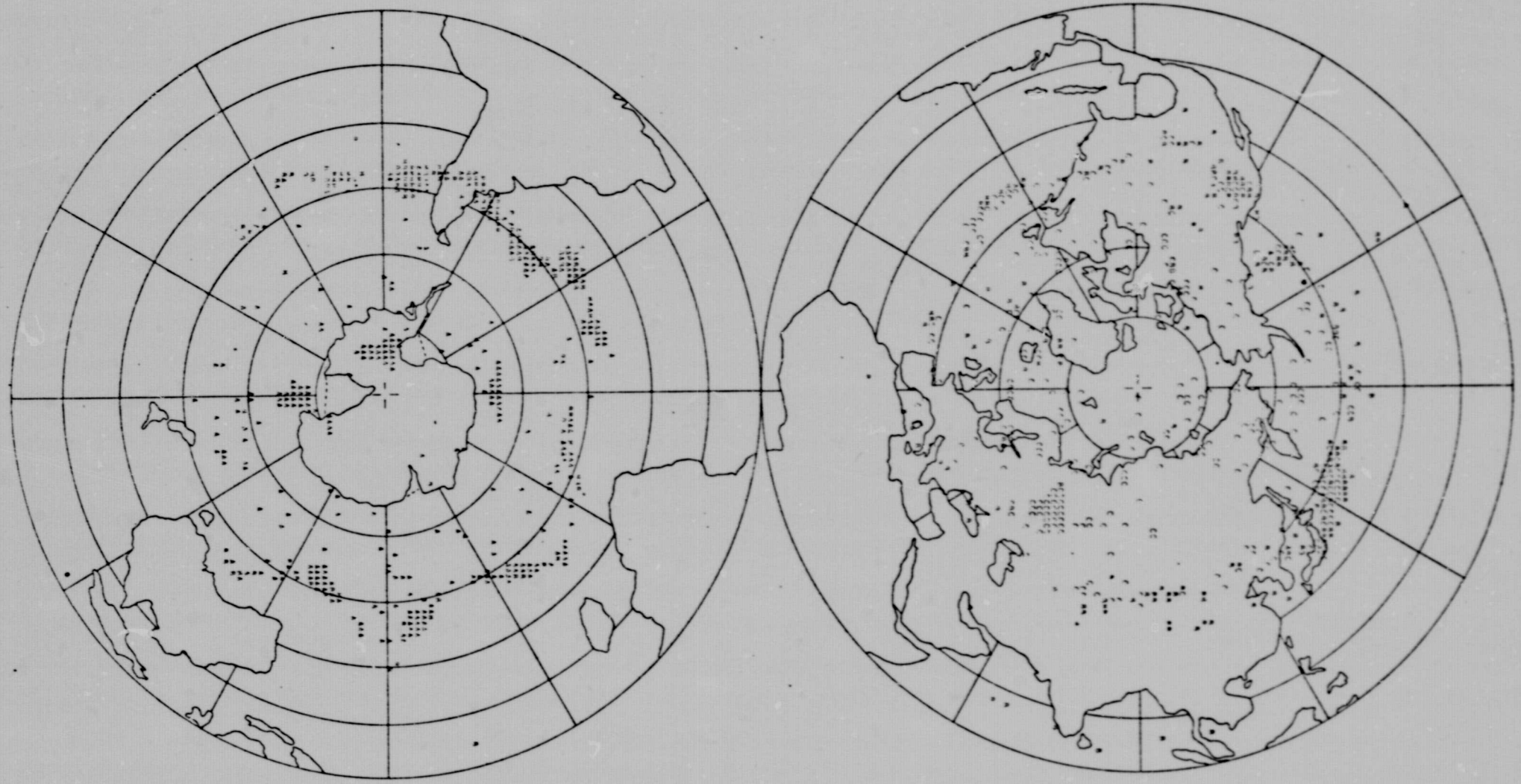

Fig. 7. Balloon positions at the upper level, on polar equal area projections, at day 60.

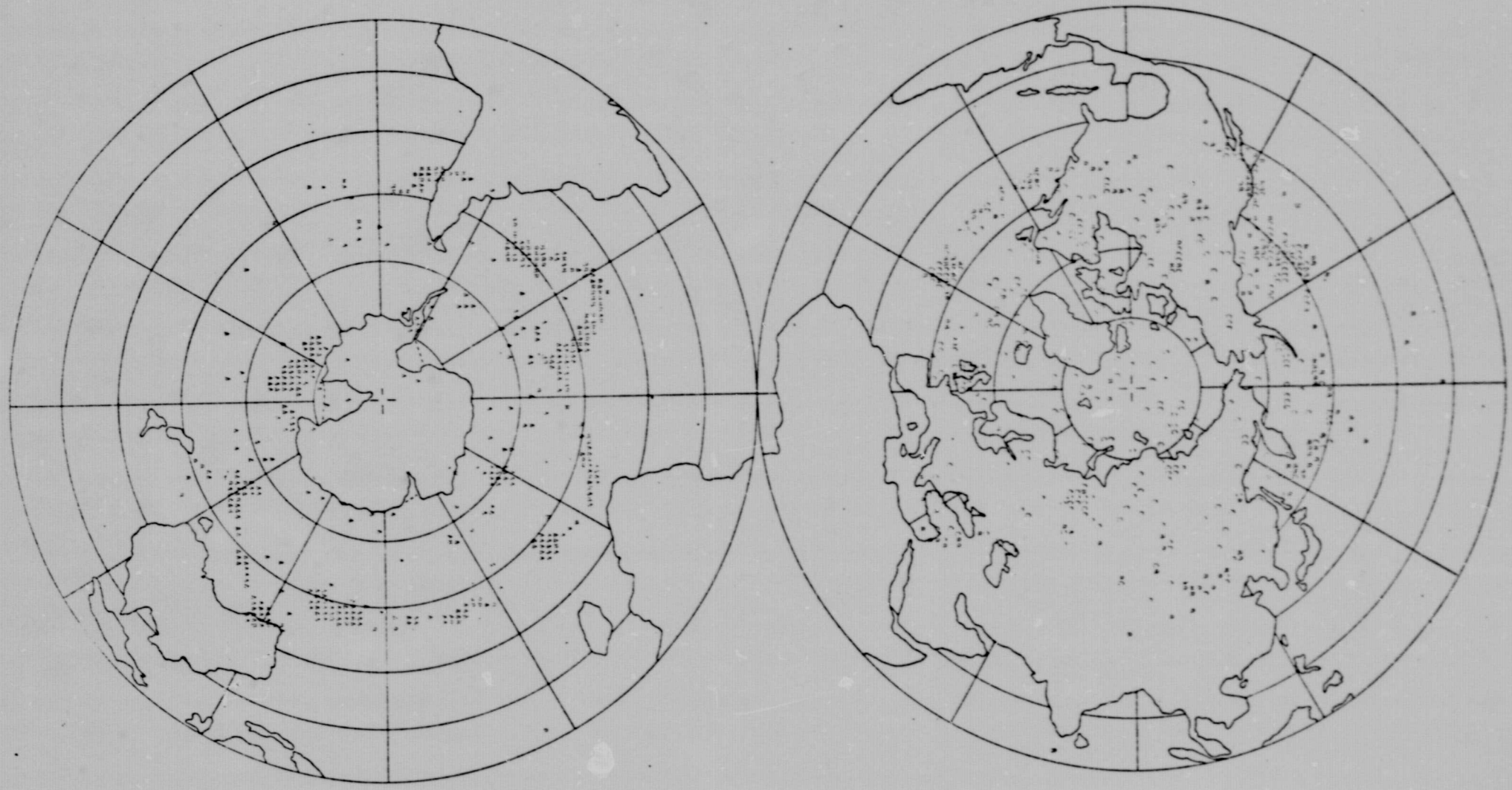

Fig. 8. Balloon positions at the upper level, on polar equal area projections, at day 70.

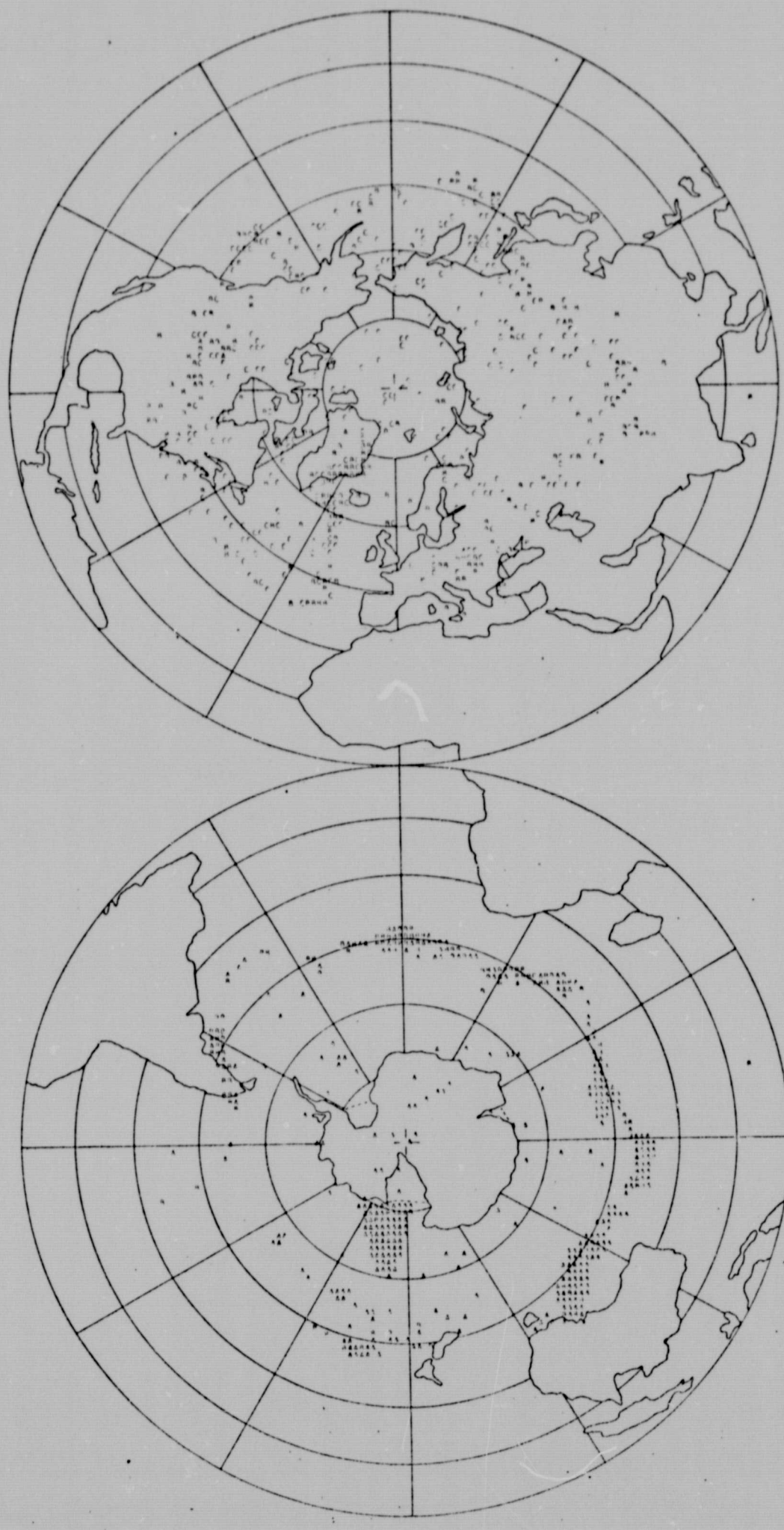

Fig. 9. Balloon positions at the upper level, on polar equal area projections, at day 80.

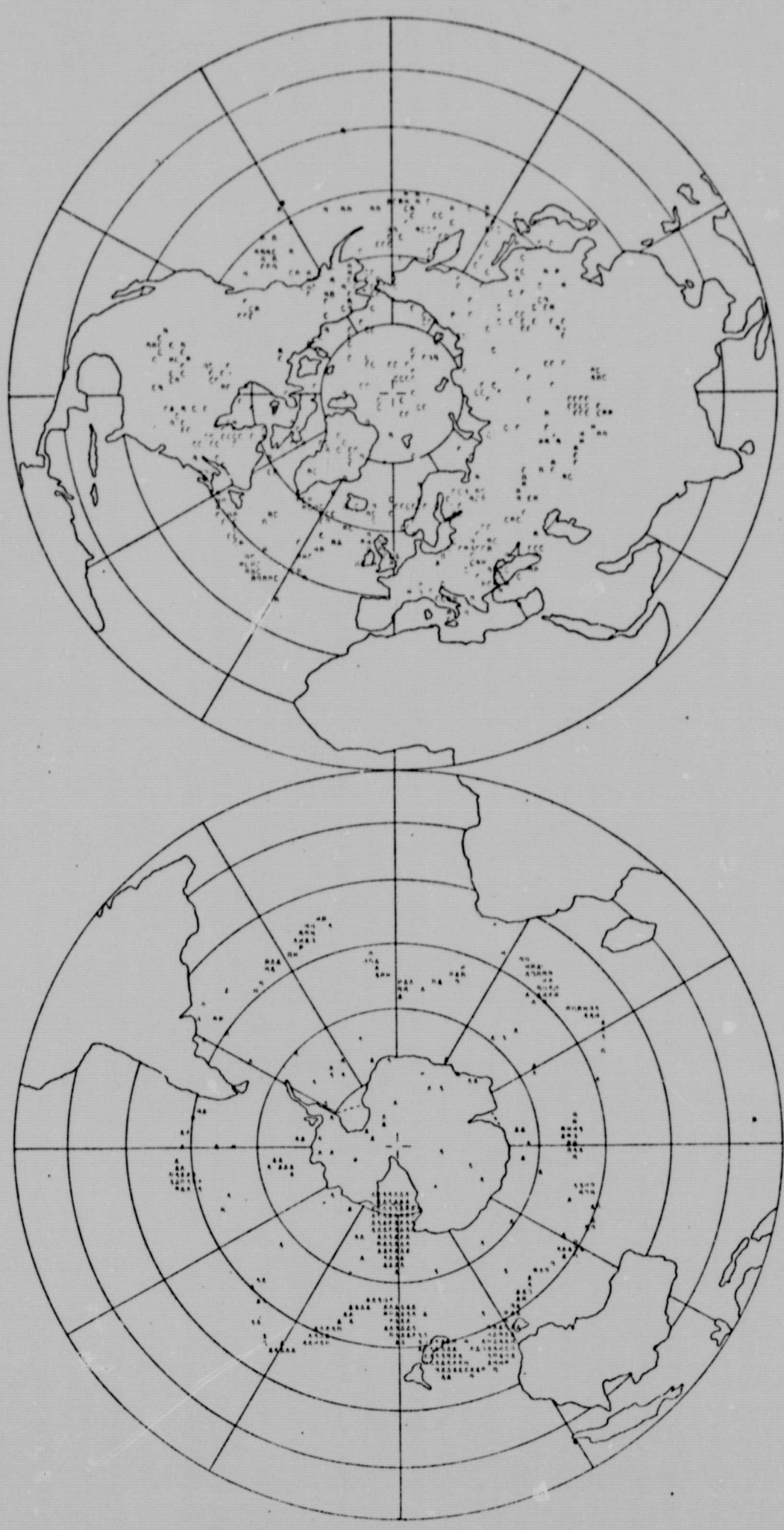

Fig. 10. Balloon positions at the upper level, on polar equal area projections, at day 90.

120°W longitude, and in the northernmost Pacific region near 180° longitude. The random distribution shown in figure 1 also has some moderate balloon clusters: for example, the one over Central America.

10 days later, as shown in figure 2, large empty regions have already appeared above the tropical continents. Also over the ocean regions, in the tropics, the number of balloons have greatly decreased. This is especially so in the central and western tropical South Atlantic.

By day 20, figure 3, the tropics as a whole have lost a large fraction of their balloons; but more remain in the central and the western tropical Pacific and the Indian Ocean than in the rest of the tropics. By day 20, some clusters have formed in the middle latitudes.

By day 30, figure 4, there is a noticeable concentration of balloons in a zone between 35°S and 45°S latitude. The same zonal concentration is found, but is not as pronounced, in the Northern Hemisphere.

From day 40 through day 90, figures 5 through 10, there is a significant slow systematic change in the balloon distributions. The middle latitude balloon concentration in the Northern Hemisphere slowly weakens, and by day 90 the balloons are well dispersed over the Northern Hemisphere middle and high latitudes. The initial transport of balloons from the tropics into the middle latitudes produced the Northern Hemisphere middle latitude concentration seen at day 40; subsequently, the dispersion process spread these balloons poleward and produced the remarkably uniform middle and high latitude distribution seen at day 90.

On the other hand, in the Southern Hemisphere the middle latitude zonal concentration persists until the end of the computation period. In addition, toward

the end of the 90 days, a pronounced cluster forms near the Ross Sea. (In our simulation of the 1970-71 Eole Experiment, a cluster also formed near the Ross Sea, at this time; but it later dispersed and was almost completely gone by day 110.)

By the end of the calculation, figure 10, there are almost no balloons in the latitudes between 30°S and 30°N.

During the computation period, from December 1, year 1, through March 1, year 2, in the model atmosphere, there is a net transport of balloons from the Southern into the Northern Hemisphere. By the end of this period, of the total of 3000 balloons there are 1638 balloons in the Northern Hemisphere and 1362 in the Southern Hemisphere. Of the 1000 balloons shown in figure 10, there are no C balloons in the Southern Hemisphere, and there are 5 A balloons in the Northern Hemisphere. Of the B balloons, 204 are in the Northern Hemisphere, and 129 are in the Southern Hemisphere. This transport of balloons, northward across the equator, takes place because the mean intertropical convergence zone is south of the equator during the period of the numerical simulation.

3. GLOBAL DISTRIBUTION OF BALLOONS IN THE LOWER TROPOSPHERE

To simulate the balloons in the lower troposphere, we use the surface of constant air density $\rho_9 = 1.114\ kg/m^3$, which is the air density at 900 mb in the Standard Atmosphere.

The initial time and the initial space distribution of the balloons, at this level, was exactly the same as that used for the balloons in upper troposphere, described in the preceding section.

By comparing the initial distribution of the balloons shown in figure 11 with those shown in figure 1, we see that of the 1000 balloons used for the figures, there are 62 balloons missing at the lower level. These are the balloons whose initial positions, on the surface ρ_9, are beneath the earth's surface. The surface ρ_9 lies below the surface of the earth where the ground elevation is high: the Himalayas, Antarctica, the Andes, western North America, and Greenland. But ρ_7 is also below the level of the ground, at more moderate elevations, where the temperature is high and/or the pressure is low for the given elevation: as, for example, in Central and South Africa.

The trajectories of the balloons at the lower level were calculated in the same way as those at the upper level, except that balloons were eliminated when they collided with the ground surface. The rate of these collisions was fairly large. Initially, 177 of the 3000 balloons (62 of the 1000 balloons used for the figures) were below ground level. But by the end of the 30 days of the trajectory calculations, a total of 997 of the 3000 balloons (335 of the 1000 balloons used for the figures) were lost by collision with the ground.

By day 10, figure 12, in addition to the initial vacant areas there are practically no balloons over central and eastern North America, South Asia, the western North Atlantic, and the Arabian Sea; and there are relatively few balloons over the tropical South Atlantic. There is an intense balloon cluster over south-central Brazil, and a moderate concentration of balloons, near the equator, in the central and western Pacific and the Indian Ocean.

About the same patterns are seen on day 20, figure 13, and on day 30, figure 14; with the cluster over south-central Brazil and the concentration near the equator, especially in the Indian Ocean, gradually becoming more intense.

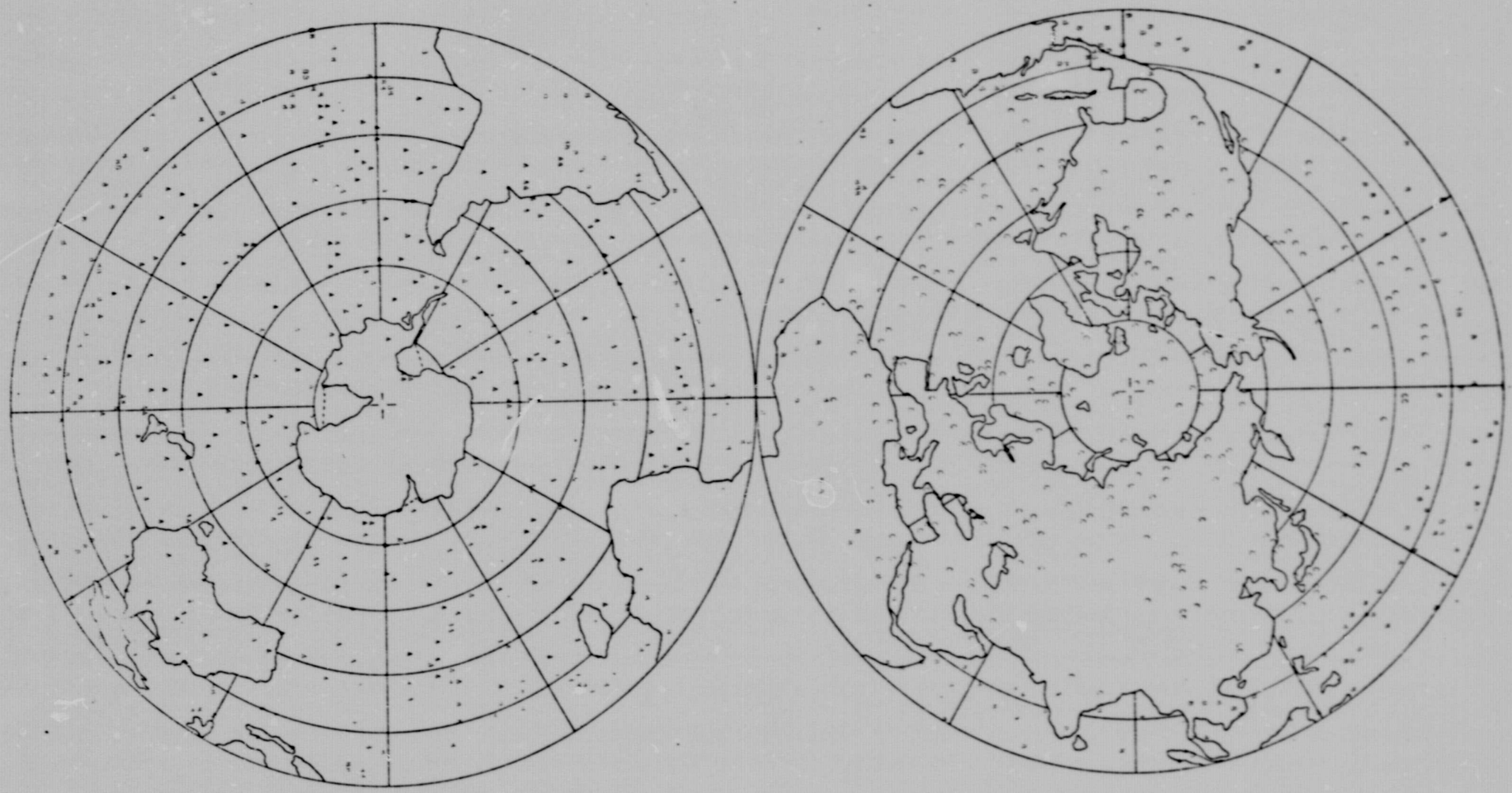

Fig. 11. Balloon positions at the lower level, on polar equal area projections, at day 0.0.

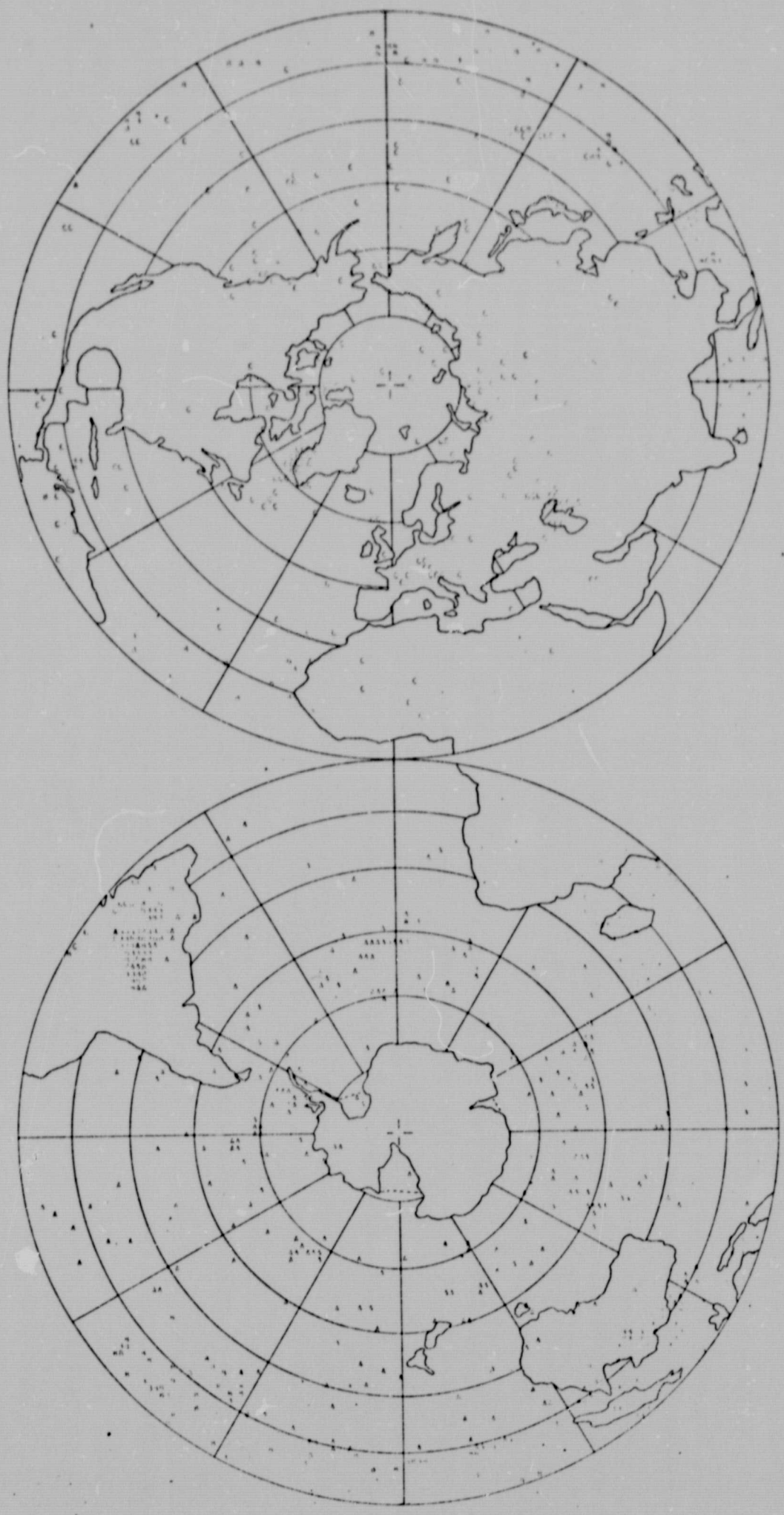

Fig. 12. Balloon positions at the lower level, on polar equal area projections, at day 10.

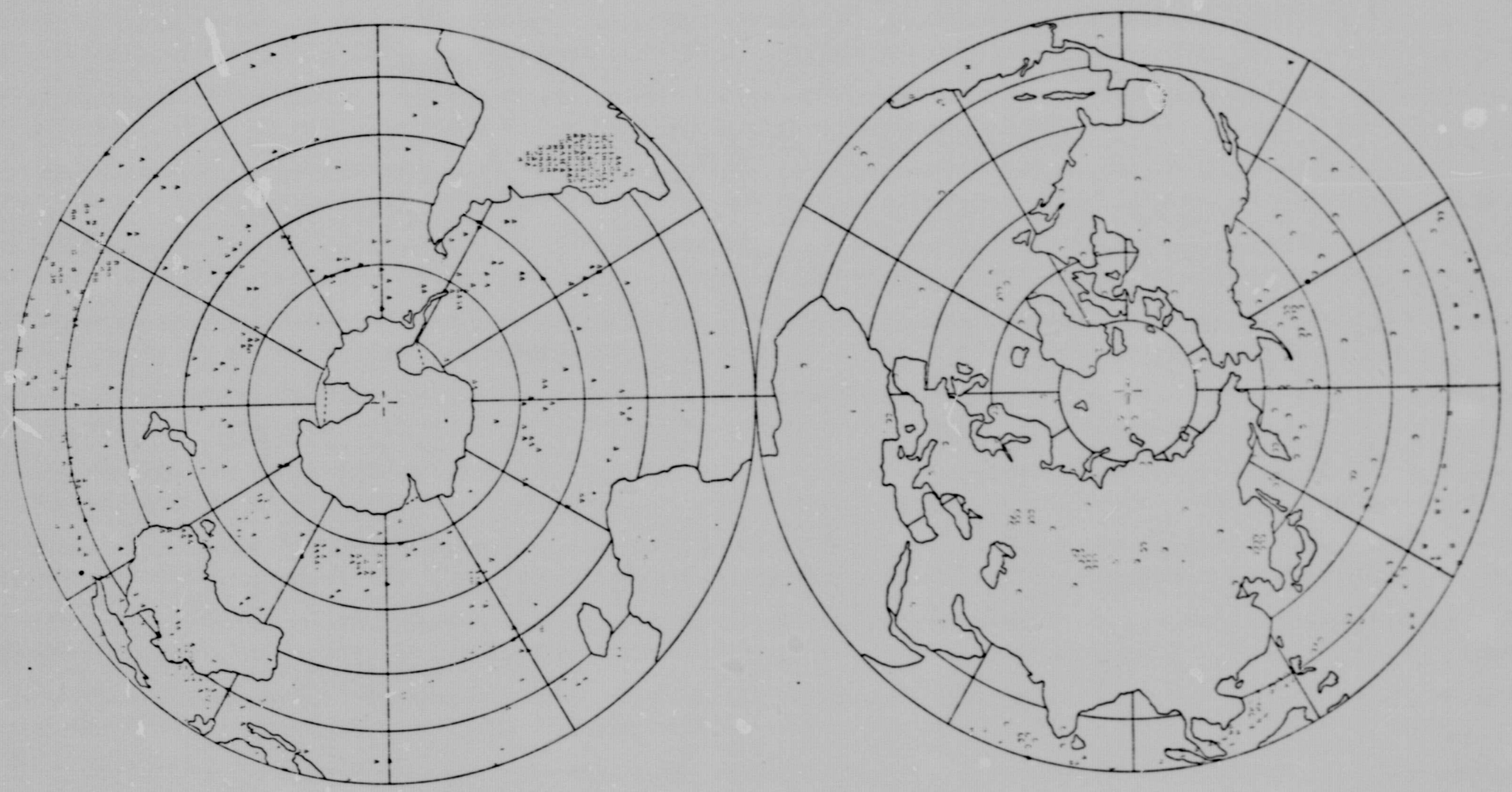

Fig. 13. Balloon positions at the lower level, on polar equal area projections, at day 20.

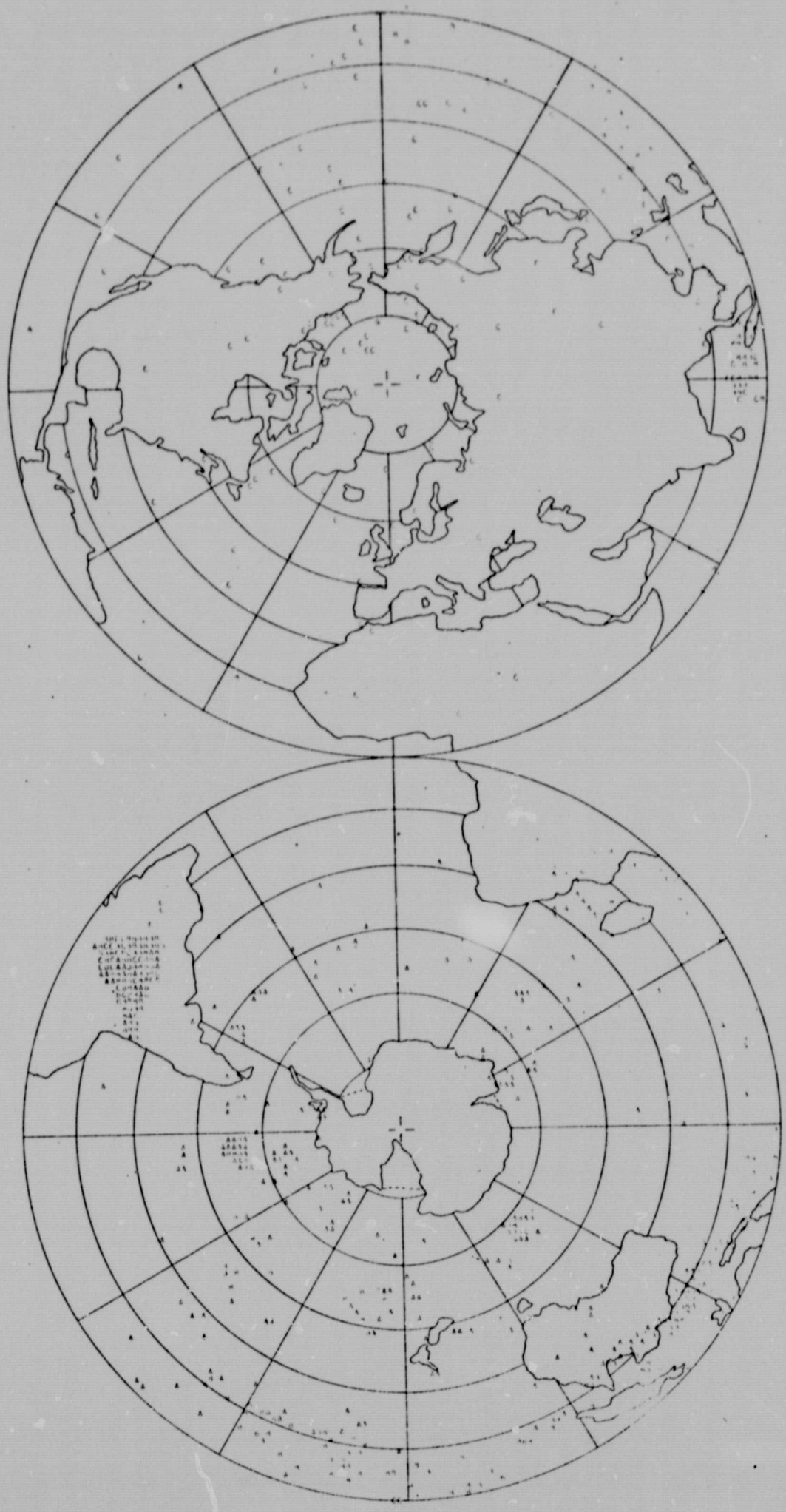

Fig. 14. Balloon positions at the lower level, on polar equal area projections, at day 30.

Because of the large loss of balloons by the topographic collisions, the numerical simulation of the balloon distributions in the lower troposphere was terminated at day 30.

Of the 2003 balloons remaining in the atmosphere on day 30, 1447 are in the Southern Hemisphere and 556 are in the Northern Hemisphere. This difference is mainly the result of the net transport of the low level balloons from the Northern into the Southern Hemisphere. To some extent it is also due to the greater rate of the topographic loss of balloons in the Northern Hemisphere. Of the total topographic loss of 997 balloons, about 60 percent is in the Northern Hemisphere.

Figure 15 shows the distribution of the 62 balloons which were initially below ground level, together with the 273 balloons which collided with the earth's surface during the subsequent 30 days. The most noticeable feature is the difference between western North America and the Himalayan region. 113 balloons in all were removed over western North America, and of these 111 were lost by collision with the ground in the 30 days that followed the initial state. On the other hand, 34 balloons in all were removed over the Himalayas, and of these only 20 were lost subsequent to the initial state. This difference indicates that the air of the lower troposphere, in the numerical model, for the most part flowed around the Himalayan topographic barrier; whereas to a much greater extent it flowed over the north-south tropographic barrier of western North America.

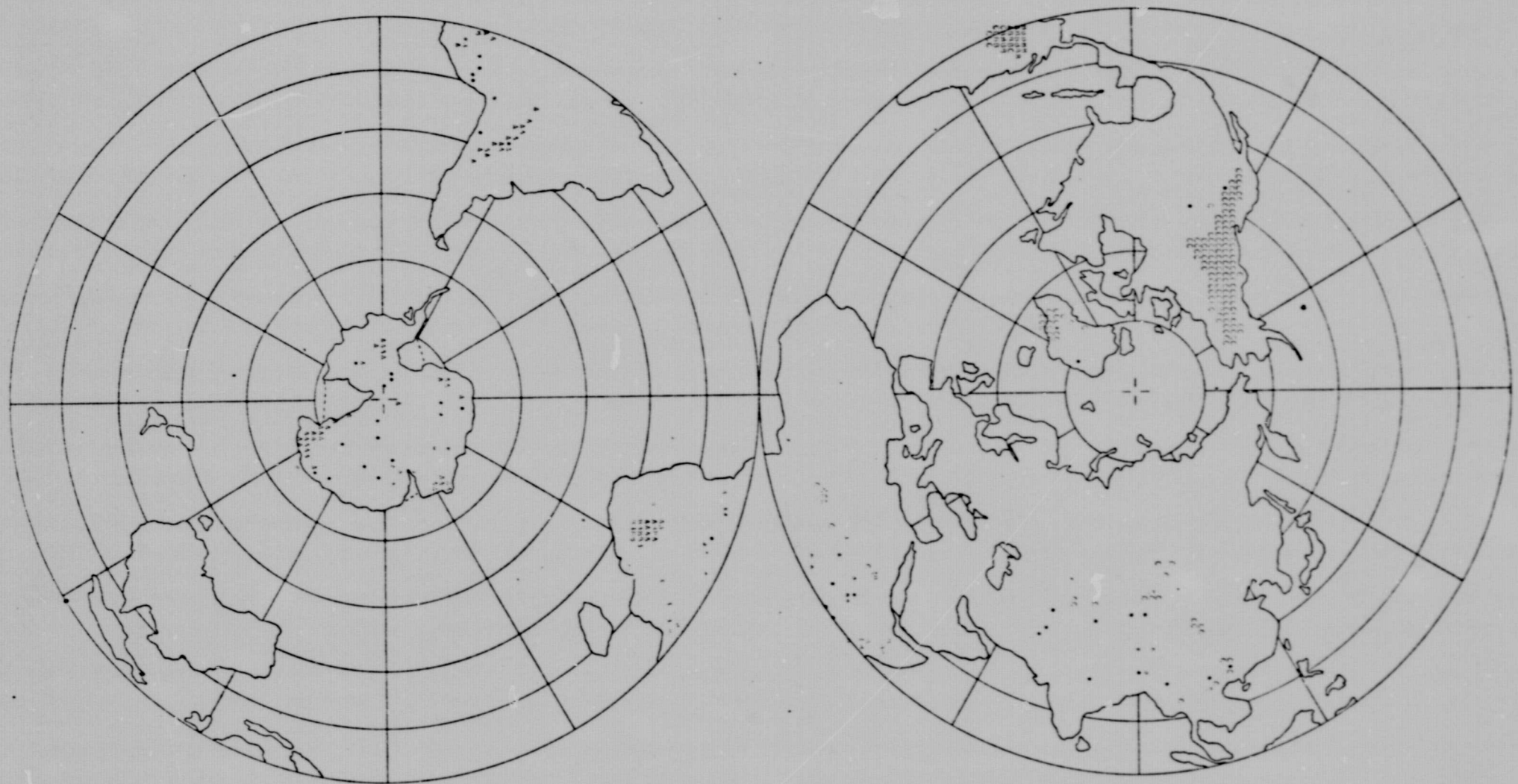

Fig. 15. Lower level balloons lost due to the earth's topography. The asterisks show balloons whose initial position on the density surface, ρ_9, was below the level of the ground. The letters show where balloons collided with the earth's surface during the subsequent 30 days.

4. STATISTICAL DESCRIPTION OF THE BALLOON DISTRIBUTIONS

In this section, we show the space-time distributions of the balloons by several different statistical representations.

To show the degree of clustering, we computed the average of the distances from a set of points to the nearest balloon. It was shown by Mesinger (1965), that if the balloons are randomly distributed with respect to one another the average nearest balloon distance has a minimum value when the balloons have a constant density in space (a constant number per unit area). This minimum value is 0.5 when the unit of length is chosen to make the average density of balloons equal to 1 per unit area. If the balloons deviate from the distribution of constant density in space, but remain random with respect to one another, the mean nearest balloon distance is larger than 0.5; and the deviation from 0.5 shows the degree of balloon clustering.

To describe the clustering in the global domain, we computed the average nearest balloon distance from 3000 points, of which 750 were randomly distributed within each one-quarter of the area of the globe, bounded by latitudes 30°S, 0°, and 30°N. Figure 16 shows this nearest balloon distance, averaged for the 3000 points, as a function of time, at both the upper and the lower levels. In this representation the unit of length is constantly adjusted to make the average density of balloons equal to 1 per unit area. The upper level curve has the initial value of 0.505. The lower level curve has the initial value of 0.544; which shows the degree of clustering due to the empty areas that occur initially where the density surface, ρ_9, is below the level of the ground.

The upper level average nearest balloon distance increases very nearly linearly with time, for the entire 90 days. The curve has not reached an equilibrium

value, because balloons are still leaving the tropical zone at the end of the 90 day period. (At day 90, 9 balloons of the 3000 are still in the region between 30°S and 30°N.)

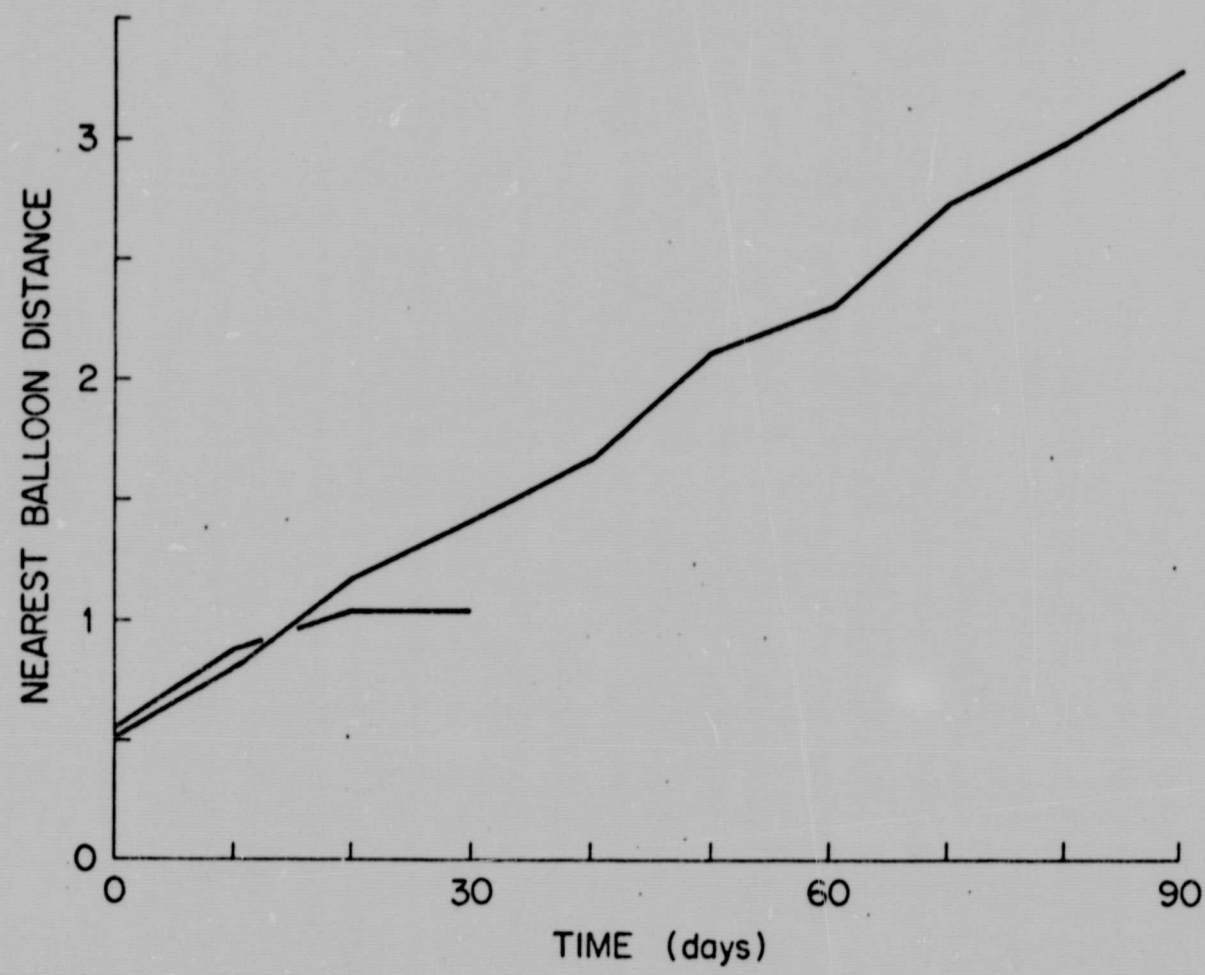

Fig. 16. Average distance to the nearest balloon from 3000 points approximately randomly distributed over the globe, at 10 day intervals. The 90 and 30 day curves are for the upper and lower levels, respectively. The unit of length is chosen to make the average density of balloons over the entire globe always equal to 1 per unit area.

The lower level average nearest balloon distance, shown in figure 16, approaches an equilibrium value of about 1.0, after about 20 days. The large difference between the behavior of upper and lower level curves reflects the fact

that the upper level is approaching the state of having no balloons within a broad tropical zone, whereas the lower level has already reached (and should maintain) the state of having many balloons near the center of this zone. On the global scale, therefore, the degree of clustering is much smaller at the lower than at the upper level.

Another statistical description of the balloon distributions is given by the histograms in figures 17 and 18. These show the distribution of the balloons with latitude, in 10° latitude intervals. Figure 17 shows the average of four histograms (for days 60, 70, 80 and 90) at the upper level. Figure 18 shows the average of two histograms (for days 20 and 30) at the lower level. The ordinate scales, in the two figures, show the density of balloons when the unit of length is again chosen such that for each individual histogram the average density of balloons over the entire globe is 1. The abscissa scales are proportional to the sine of the latitude.

Figure 17 shows almost no balloons in the broad zone between 30°S and 30°N. In the Southern Hemisphere there is a narrow zone of maximum density of balloons near 45° latitude; and a secondary maximum in the polar region. This distribution shows the effect of the upper tropospheric convergence and divergence of a three cell mean meridional circulation. In the Northern Hemisphere the balloon distribution, poleward of 30° latitude, is much more uniform. This shows that the dispersion of the balloons, produced by the deformation fields of the disturbances, is more effective (relative to the Ferell cell circulation) in the Northern than in the Southern Hemisphere.

At the lower level, figure 18 shows three zones of maximum balloon density: one at the intertropical convergence zone, the second centered at 55°S latitude, and the third centered at 55°N latitude. It also shows more balloons in

the Southern than in the Northern Hemisphere. As indicated in section 3, the main reason for the asymmetry is the cross-equatorial transport of the balloons.

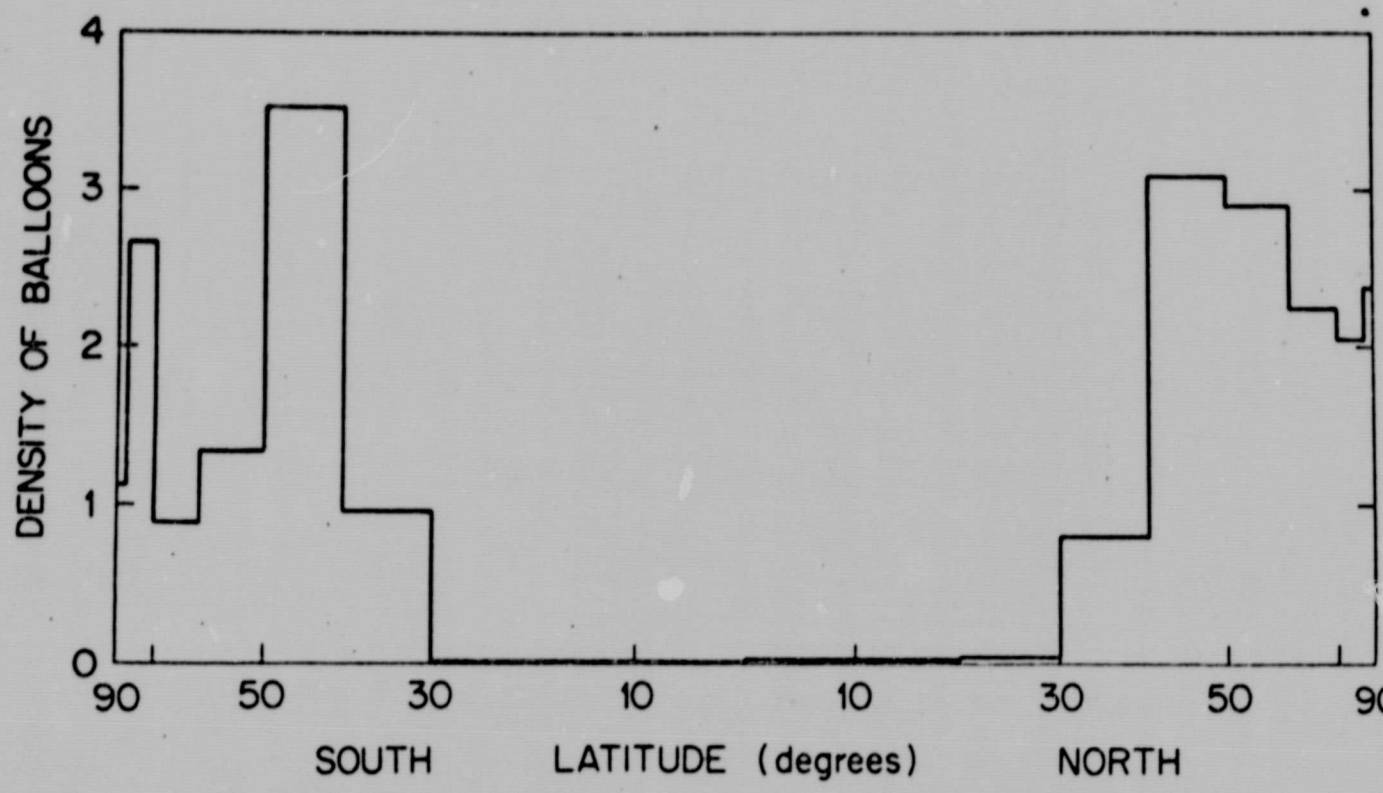

Fig. 17. The upper level average density of balloons (the number per unit area), in each ten degree latitude zone, averaged for the last 30 days. The abscissa scale is proportional to the sine of the latitude. The ordinate scale gives the density of balloons when the unit of length is chosen to make the average density of balloons over the entire globe equal to 1 per unit area.

Figure 17 shows that after day 60 almost all of the upper level balloons are in the regions poleward of 30° latitude, in the two hemispheres. It is useful, therefore, to see how the nearest balloon distance, of which only the global average value was shown in figure 16, will appear when the two regions poleward of 30°S

and 30°N latitude, and the larger region between 30°S and 30°N latitude, are considered separately. We shall refer to these three regions as the Southern (S), the Tropical (T), and the Northern (N) regions.

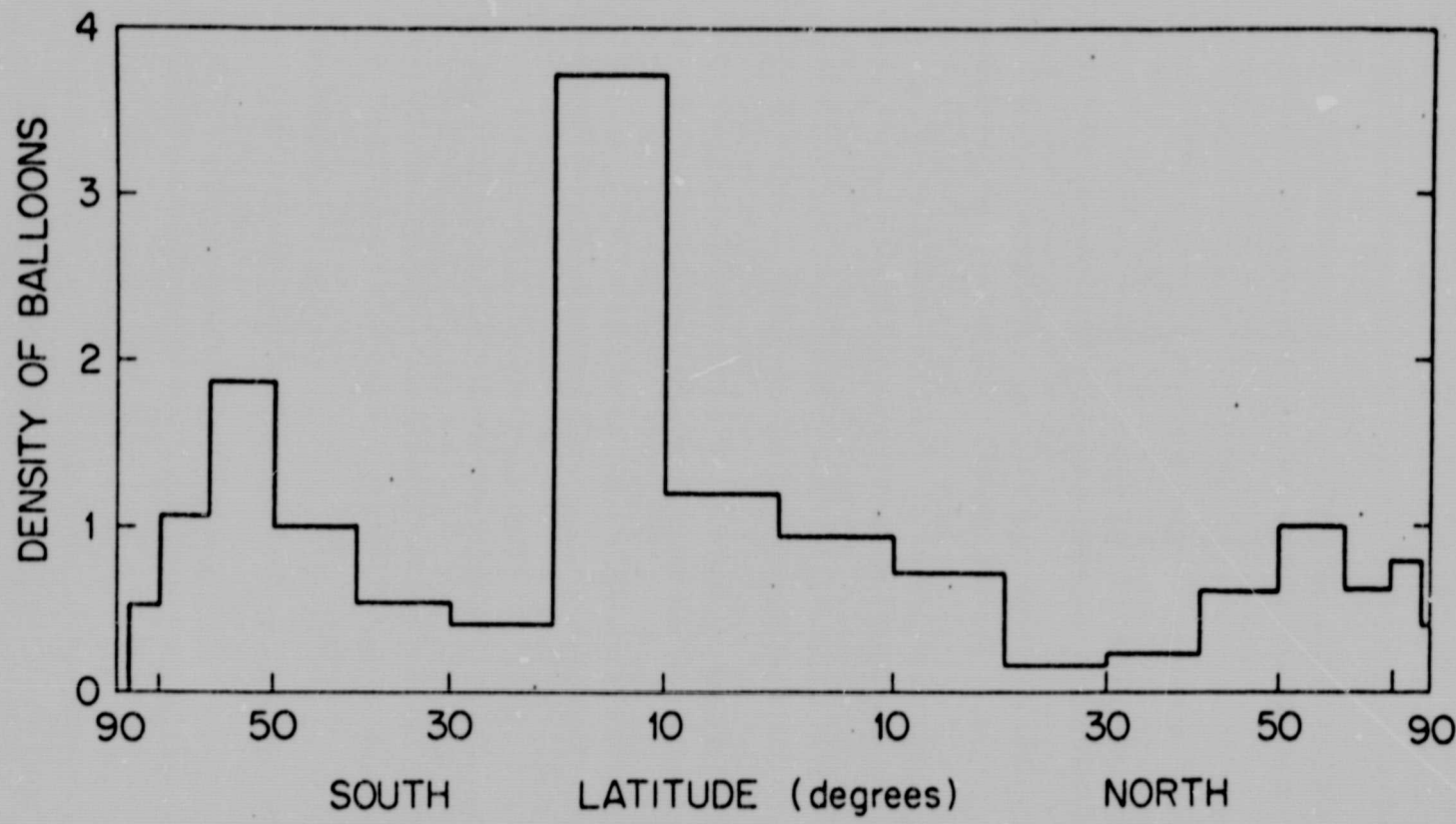

Fig. 18. The lower level average density of balloons (the number per unit area), in each ten degree latitude zone, averaged for the last 10 days. The abscissa scale is proportional to the sine of the latitude. The ordinate scale gives the density of balloons when the unit of length is chosen to make the average density of balloons over the entire globe always equal to 1 per unit area.

Figure 19 shows the average nearest balloon distance for each of the three regions, and at the two levels. The unit of length used for calculating the nearest balloon distance is the same as the one used for figure 16. It is constantly adjusted to the total number of balloons, for each level, and does not depend on the number of balloons in each particular region. This was done in order to show how the average nearest balloon distance, in each of the three regions, contributes to the global average shown in figure 16.

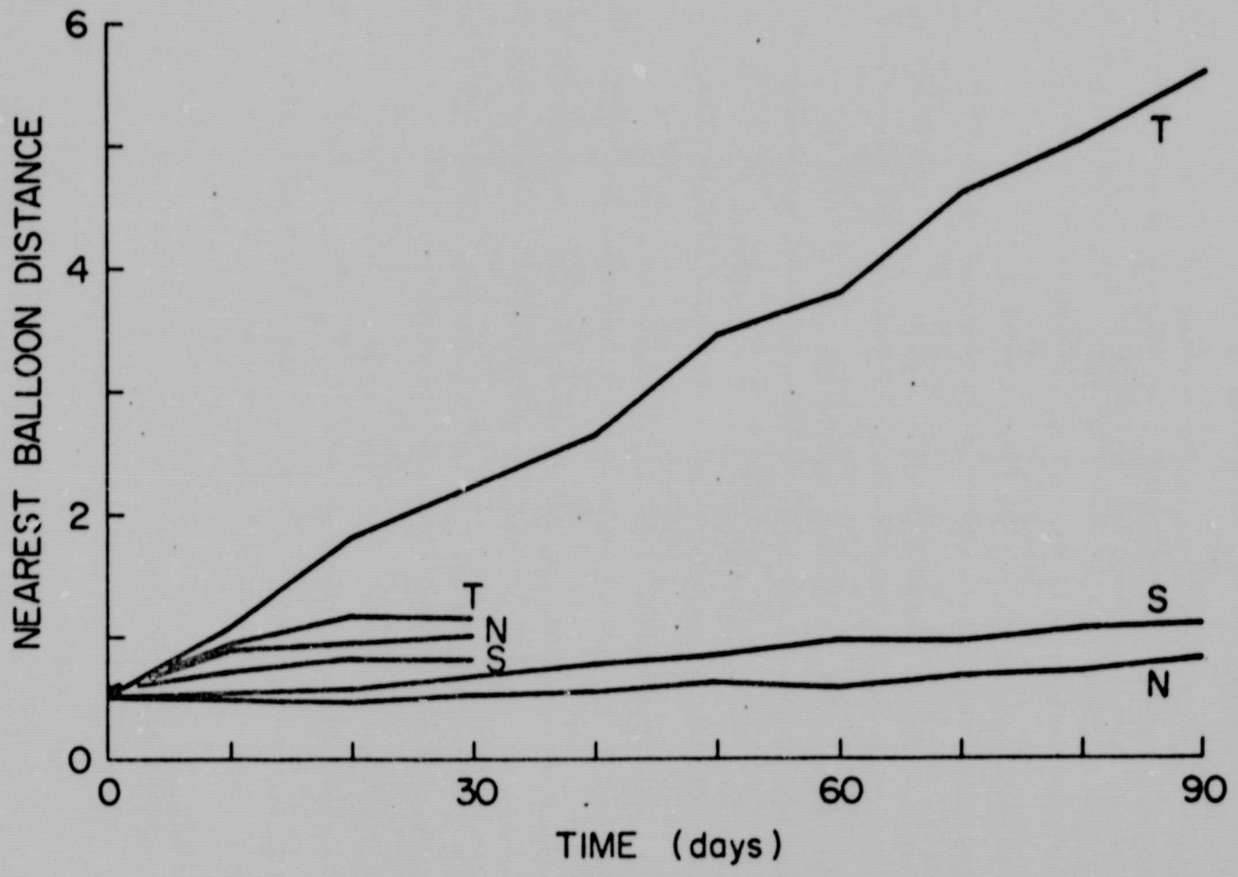

Fig. 19. Average distance to the nearest balloon for each of the three regions: S(90°S to 30°S), T(30°S to 30°N), and N(30°N to 90°N), at 10 day intervals. The 90 and 30 day curves are for the upper and lower levels, respectively. The unit of length is chosen to make the average density of balloons over the entire globe always equal to 1 per unit area.

We see that almost the entire linear growth of the global average nearest balloon distance, at the upper level, was produced by the steady growth in the Tropical region. This growth is a result of the constant decrease of the number of balloons in that region. In the Southern and Northern regions there are only small rates of increase of the average nearest balloon distance: in the Southern region the change is from 0.50 to 1.11, and in the Northern region from 0.50 to 0.84, over the 90 day period. These curves show that within the Southern and Northern regions the increase in the number of balloons on the whole is less effective in reducing the average nearest balloon distance, than is the clustering within these regions in increasing the average nearest balloon distance.

For the lower level, figure 19 shows that the nearest balloon distance in the Tropical region is only slightly greater than that of the two polar regions. The Southern region has the smallest nearest balloon distance. As we shall see in the analysis which follows, this is due to the larger number of balloons in the Southern region, rather than to a more uniform distribution of the balloons.

Figure 20 shows the average nearest balloon distance, when the unit of length is continuously adjusted to the number of balloons at each level and within each of the three regions. The adjustment is done so as to make the averate density of balloons within each region always equal to 1 per unit area. Therefore, these curves show the degree of balloon clustering in each of the regions.

We see that at the upper level the balloons cluster, in both the Northern and Southern regions, throughout the 90 day period. In the Southern region, this clustering is mainly the result of the accumulation of balloons in the zone centered at 45°S latitude (cf. figures 1 through 10). In the Northern region, on the other hand, the clustering shown in figure 20 is mainly the result of the growing depletion of balloons in the latitude zone 30°N to 40°N. This depletion dominates over the

fact that, during the last part of the period, the balloons become more uniformly distributed poleward of 40°N latitude. In the Tropical region, the average nearest balloon distance, at the upper level, decreases from about day 20 on. This has no practical significance; because the total number of balloons within the region becomes very small, and the sampling error large.

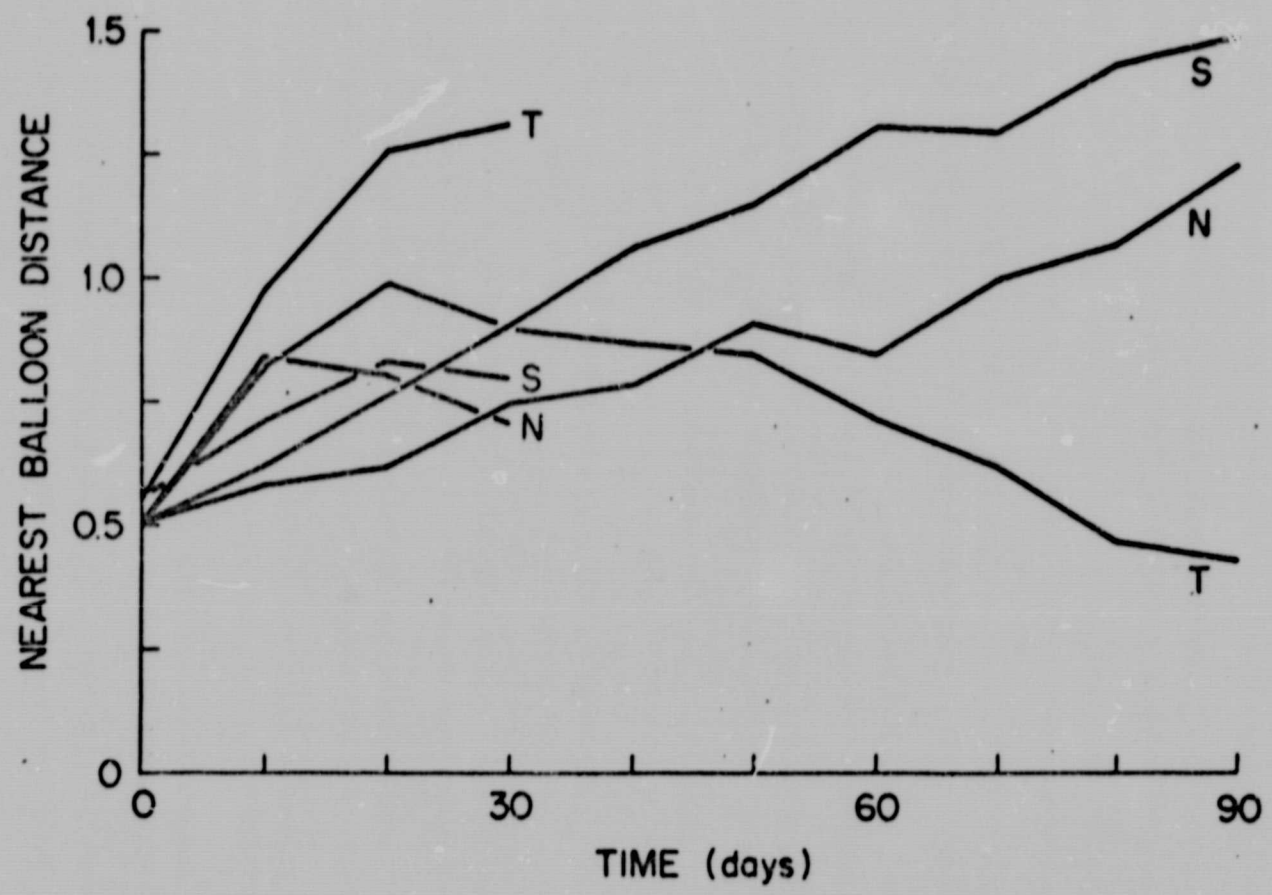

Fig. 20. Average distance to the nearest balloon for each of the three regions: S(90°S to 30°S), T(30°S to 30°N), and N(30°N to 90°N), at 10 day intervals. The 90 and 30 day curves are for the upper and lower levels, respectively. The unit of length is continuously adjusted to the number of balloons within each of the three regions, so as to make the average density of balloons within each region always equal to 1 per unit area.

At the lower level, the rate of clustering is very large in the Tropical region. In the Northern and Southern regions, the clustering stops before the end of the 30 day period. The fact that the Northern region ends with the smallest

value of the nearest balloon distance, in this representation, shows that the balloons are more uniformly distribured there than in the other two regions.

Figure 21 shows the total global topographic loss of balloons, at the lower level, as a function of time. In general, the rate of loss decreases with time because the total number of balloons is decreasing.

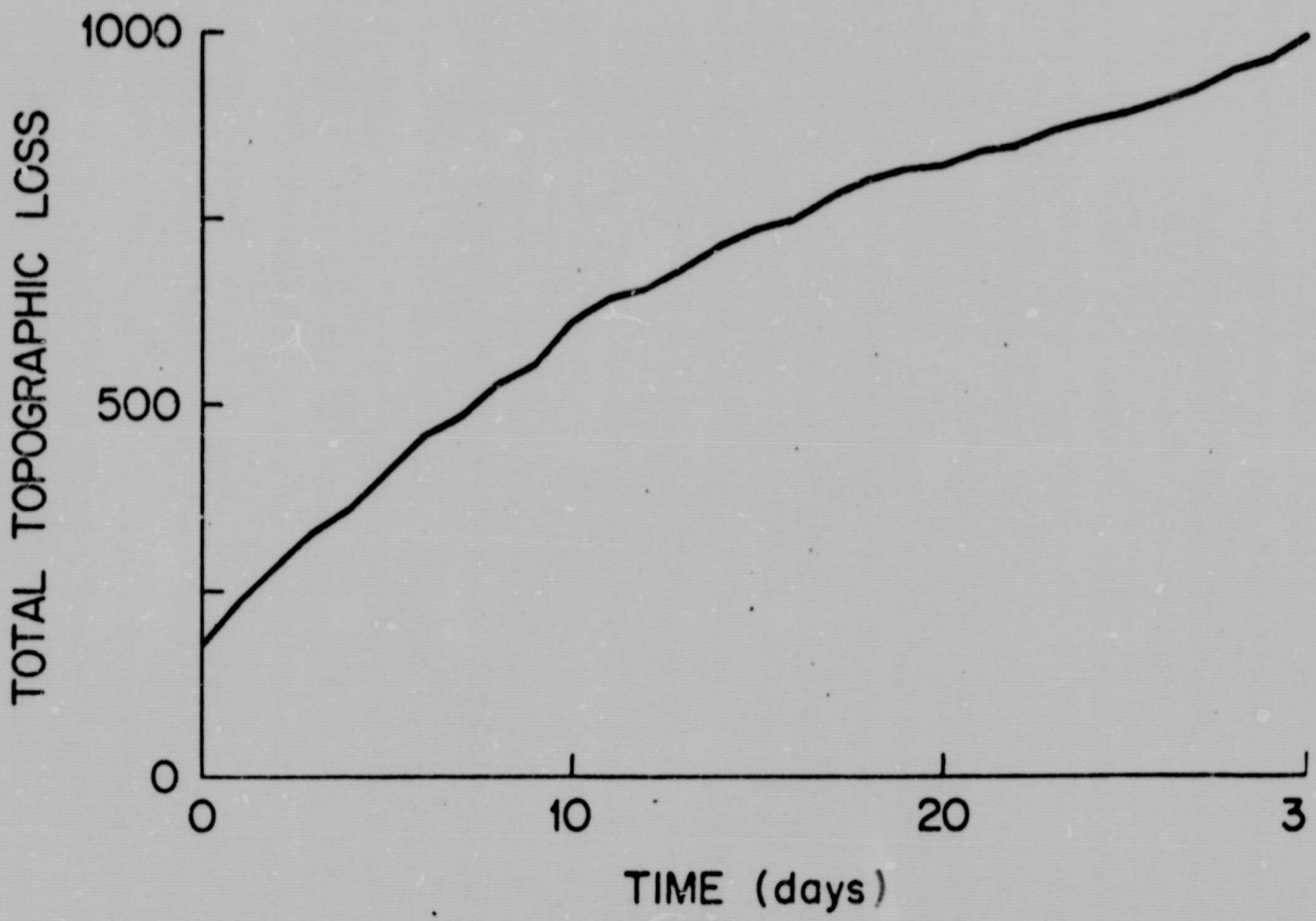

Fig. 21. The total topographic loss of balloons at the lower level, as a function of time.

5. SUMMARY AND CONCLUSIONS

In our numerical simulation of the clustering of constant-volume balloons in the global domain, we found that starting with an ideal distribution of balloons which are approximately randomly spaced over the globe, in the upper troposphere the balloons rapidly leave the Tropical region. From an initial 1500 balloons between 30°S and 30°N latitude, the number decreases to 250 by day 30, to 53 by day 60, and to 9 balloons by day 90. We must point out, however, that the test comparison between observed and simulated GHOST balloons, given in the preceding report (Mesinger and Mintz, 1970), indicated that a smaller rate of depletion of balloons from the Tropical region should occur in the real atmosphere.

In the Southern and Northern regions poleward of 30°S and 30°N latitudes, there is the corresponding increase in the number of balloons at the upper level; more of them going into the Northern region at this season of the year (December, January, February). But in spite of the approximate doubling of the number of balloons in the Northern and Southern regions by day 90, there was approximately a doubling of the average nearest balloon distance, within these regions, due to the clustering of the balloons. In the Southern region, the clustering consisted mainly of the accumulation of balloons in a relatively narrow zone centered at 45°S latitude. In the Northern region, the balloons toward the end of the period became rather uniformly distributed poleward of 40°N latitude, but there was a depletion of balloons in the zone 30°N to 40°N.

In the lower troposphere, at the density surface corresponding to 900 mb in the Standard Atmosphere, there was a rapid loss of balloons by collision with the earth's surface: about one-third of the initially approximately randomly distributed balloons were lost, in this way, in 30 days. Of the balloons that remained, many collected along the intertropical convergence zone, with a very large cluster over

south-central Brazil. The smaller number of balloons that remained in the Northern region, in the lower level, were rather well distributed: but in our numerical simulation we did not subject the balloons to failure by icing in super-cooled water clouds.

6. ACKNOWLEDGMENTS

The research reported here was done with the support of the National Aeronautics and Space Administration, NASA Grant No. NGR 05 007 091.

The wind and mass fields used to simulate the constant-volume balloon trajectories were taken from a research project on Numerical Simulation of the General Circulation of the Atmosphere, supported by the Atmospheric Sciences Section, National Science Foundation, NSF Grant GA-1470.

REFERENCES

Angell, J. K. and Hass, W. A., 1966: Effect of Clustering upon a 500-mb Horizontal Sounding System. Mon. Wea. Rev., Vol. 94, pp. 151-166.

Arakawa, A., Katayama, A. and Mintz, Y., 1969: Numerical Simulation of the General Circulation of the Atmosphere. Proceedings of the WMO/IUGG Symposium on Numerical Weather Prediction in Tokyo, November 26-December 4, 1968, Technical Report of the Japan Meteorological Agency No. 67, pp. IV-7 - IV-8-12.

Lally, V. E. and Lichfield, E. W., 1969: Summary of Results and Plans for the GHOST Balloon Project. Bull. Amer. Meteor. Soc., Vol. 50, pp. 867-874.

Mesinger, F., 1965: Behavior of a Very Large Number of Constant-Volume Trajectories. J. Atmos. Sci., Vol. 22, pp. 479-492.

Mesinger, F. and Mintz, Y., 1970: Numerical Simulation of the 1970-71 Eole Experiment. Numerical Simulation of Weather and Climate, Technical Report No. 4, Department of Meteorology, University of California, Los Angeles, 51 pp.

Mintz, Y., 1965: Very Long Term Global Integration of the Primitive Equations of Atmospheric Motion. (An Experiment in Climate Simulation.) WMO-IUGG Symposium on Research and Development Aspects of Long Range Forecasting, Boulder, Colo., 1964, World Meteorological Organization, Technical Note No. 66, pp. 141-167; (and Meteor. Monographs, Vol. 8, No. 30, pp. 20-36, 1968).

Morel, P., 1969: Constant Level Balloon Flights Program in France. Laboratoire de Météorologie Dynamique, Centre National de la Recherche Scientifique, France, Report No. 6, 37 pp.

NAS-NRC Panel on International Meteorological Cooperation, 1966: The Feasibility of a Global Observation and Analysis Experiment. National Academy of Sciences - National Research Council, Publication 1290, 172 pp.

Solot, S. B., 1968: GHOST Balloon Data, Vols. 1-11. National Center for Atmospheric Research, Boulder, Colo., Technical Note No. 34.

WMO-ICSU Joint Organizing Committee, 1969: The Planning of the First GARP Global Experiment. GARP Publications Series, No. 3, World Meteorological Organization, Geneva, 36 pp.